

Portland State University

PDXScholar

Physics Faculty Publications and Presentations

Physics

6-28-2024

Monitoring Water Meniscus Formation at Nanocontacts with Shear-Force Acousto Near-Field Microscopy

Xiaohua Wang

Portland State University

Rodolfo Fernandez

Portland State University

Theodore Brockman

Portland State University

Kacharat Supichayangoon

Portland State University

Andres H. La Rosa

Portland State University

Follow this and additional works at: https://pdxscholar.library.pdx.edu/phy_fac



Part of the [Physics Commons](#)

Let us know how access to this document benefits you.


Citation Details

Wang, X., Fernandez, R., Brockman, T., Supichayangoon, K., & La Rosa, A. H. (2024). Monitoring water meniscus formation at nanocontacts with shear-force acousto near-field microscopy. *Journal of Applied Physics*, 135(24).

This Article is brought to you for free and open access. It has been accepted for inclusion in Physics Faculty Publications and Presentations by an authorized administrator of PDXScholar. Please contact us if we can make this document more accessible: pdxscholar@pdx.edu.

RESEARCH ARTICLE | JUNE 27 2024

Monitoring water meniscus formation at nanocontacts with shear-force acousto near-field microscopy

Xiaohua Wang; Rodolfo Fernandez; Theodore Brockman; Kacharat Supichayangoon; Andres H. La Rosa 



J. Appl. Phys. 135, 244702 (2024)

<https://doi.org/10.1063/5.0215054>



Journal of Applied Physics

Special Topic:

Phonon-Magnon Interactions:
From Fundamentals to Device Physics

Guest Editors: Vasily V. Temnov, Alexey V. Scherbakov, Yoshi Chika Otani, Paolo Vavassori

Submit Today!

Monitoring water meniscus formation at nanocontacts with shear-force acousto near-field microscopy

Cite as: J. Appl. Phys. 135, 244702 (2024); doi: 10.1063/5.0215054

Submitted: 22 April 2024 · Accepted: 5 June 2024 ·

Published Online: 27 June 2024



Xiaohua Wang,¹ Rodolfo Fernandez,¹ Theodore Brockman,¹ Kacharat Supichayanggoon,¹
and Andres H. La Rosa^{1,2,a)} 

AFFILIATIONS

¹Department of Physics, Portland State University, P.O. Box 751, Portland, Oregon 97207, USA

²Physics Department, National University of Engineering, Lima, Peru

^{a)}Author to whom correspondence should be addressed: andres@pdx.edu

ABSTRACT

Shear-force acoustic near-field microscopy (SANM) is employed to monitor stochastic formation and post dynamic response of a water meniscus that bridges a tapered gold probe (undergoing lateral oscillations of a few nanometers amplitude at constant frequency) and a flat (gold or silicon oxide) substrate. As the probe further approaches the substrate, its amplitude decreases. Shear forces (of yet unknown precise origin) are typically invoked to explain the apparently pure damping effects affecting the probe's motion. Herein, SANM measurements underscore instead the role of near-field acoustic emission from the water meniscus as an elastic energy dissipation channel involved in shear interactions. A simplified thermodynamic argument is provided to justify the formation of a water meniscus between the probe and the sample once they are at sufficient separation distance. The reported measurements focus on the role played by the tip's geometry (by using probes of slender and chubby apex termination). The results shed some light on the potential origin of the so-called shear forces, invoked in many scanning probe microscopy applications, but not yet well understood.

© 2024 Author(s). All article content, except where otherwise noted, is licensed under a Creative Commons Attribution-NonCommercial 4.0 International (CC BY-NC) license (<https://creativecommons.org/licenses/by-nc/4.0/>). <https://doi.org/10.1063/5.0215054>

I. INTRODUCTION

Investigation into the unusual viscoelastic properties (different from the bulk)^{1,2} displayed by mesoscopic water menisci—that spontaneously forms at ambient conditions when a sharp probe is placed in close proximity to a flat substrate—is relevant to a variety of technological areas, including adhesion,^{3,4} wetting processes,⁵ and interfacial (i.e., wearless) friction phenomena.^{6–8} Several techniques have significantly contributed to the study of this type of mesoscopic fluids,^{9–11} but information about the nature of *probe–fluid–substrate* interactions is typically inferred only from the mechanical response of the participating *probe*.^{12,13} An independent monitoring of the *fluid's* response would be ideal. Herein, the capabilities of shear-force acoustic near-field microscopy (SANM)¹⁴ for monitoring the near-field¹⁵ acoustic emission from the fluid meniscus are demonstrated, thus accounting for an elastic (i.e., reversible) energy dissipation channel in shear interactions. Focus is placed on the role played by the geometry of the probe in

the SANM measurements, for which results obtained using slender and chubby tapered probes will be contrasted. In general, the manuscript underscores the potential benefits of having an extra sensing mechanism (the near-field acoustic emission) to characterize confined mesoscopic fluids under shear.

II. SANM EXPERIMENTAL DETAILS

Tapered probes were fabricated using gold wires of 100 μm diameter through electrochemical etching procedures.¹⁶ Monolayer patches of water are expected to cover a gold surface at 35% relative humidity.¹⁷ The experiments are performed at ambient conditions with the probe, the sample, and the vertical-scanner stage inside an acrylic enclosure, which serves both to keep clean the region of measurements and to set the humidity under controlled pumping of DI water vapor and nitrogen gas. Wetting properties of the probe (gold is reported to be hydrophilic¹⁸ but it is affected by the adhesion of hydrocarbons present in the ambient) are verified by immersing the

17 July 2024 16:02:22

back cylindrical section of the gold probe into a macroscopic drop of water; a 90° contact angle is observed. This type of hydrophobic probe is used in the experiments reported herein.¹⁹ A tapered probe is mounted to one of the prongs of a 32 kHz quartz tuning fork (QTF), with the apex protruding less than 1 mm beyond the prong's edge. A silicon wafer (with its naturally grown oxide) was cleaned in Piranha solution and dried under N_2 , which rendered a sample of the hydrophilic character.²⁰ The experiments are performed at 25% relative humidity, at which ~ 2 monolayers of icelike water are expected to cover the silicon oxide surface at room temperature.²¹ The sample is placed on top of an acoustic sensor.²²

The experimental setup is schematically presented in Fig. 1. Vertical position control of the probe is implemented using a piezo-actuated nanopositioner.²³ A quartz tuning fork (QTF) of 32 kHz nominal frequency, with a tapered probe mounted to one of the prongs, is electrically driven at its resonance frequency (initially measured when the probe is far away from the sample); its piezoelectric current ΔI response is synchronously detected (lock-in #1, SR850 Stanford Research System), which is used to estimate the probe's amplitude of oscillations.^{24,25} At a certain probe-sample distance d , while the probe is approaching the sample, a water meniscus bridge stochastically forms (typically $d \sim 20$ nm, but depending on the humidity), which generates an acoustic wave that couples into the millimeter-thick substrate and travels down to the acoustic sensor (located in mechanical contact with the back side of the sample, thus in a near-field detection region).¹⁵ The output current signal from the acoustic sensor is synchronously detected (lock-in #2 in Fig. 1). As the tip further approaches the sample, changes in the QTF signal (the probe's amplitude) reflect the effect of shear interaction *on the tip*, while the simultaneously recorded changes of the SANM acoustic signal reflects the effects of shear interaction *on the confined mesoscopic fluid*. Overall, since the complexity of the probe-fluid-substrate interactions may depend on several factors (including the environment humidity, the wetting

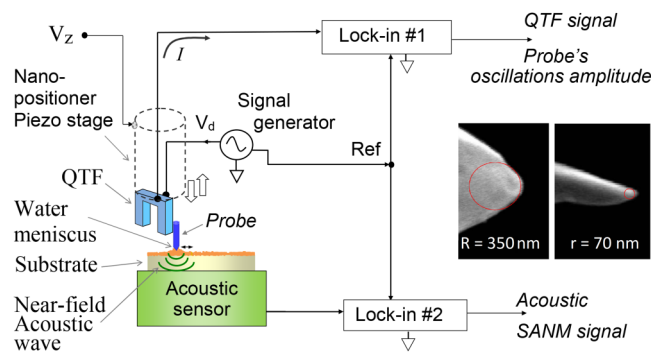


FIG. 1. Schematic of the SANM experimental setup used to independently, but simultaneously, monitor both (a) the probe's lateral oscillation amplitude (QTF signal) and (b) the near-field acoustic wave emitted by the fluid meniscus that bridges the tapered probe and the flat substrate (SANM signal), at different probe-sample separation distances. Inset: images of the chubby and slender tapered gold probes (of apex's radius of curvature $R = 350$ nm and $r = 70$ nm, respectively) used in these experiments.

properties of the surfaces, and the velocity of the tip's vertical motion), herein, the measurements focus on the impact produced by changes in the gold tip's geometry upon approaching a flat hydrophilic silicon oxide substrate.

III. RESULTS AND DISCUSSIONS

A. Control experiment: Conducting probe and conducting sample

First, a control experiment is implemented with an electrically biased (50 mV) gold probe and a grounded conducting sample,²⁶ which (a) will allow to more precisely identify the location of the substrate in an approach-retraction signal trace (contact current should be detected when the probe mechanically touches the substrate during the approach), and consequently, (b) would help recognize how a near-field acoustic trace behaves near a substrate. (In this control experiment, the probe fabrication followed a regular procedure used in our laboratory that renders a probe of typical ~ 200 nm apex radius, different than the specific fabrication steps taken to obtain the very slender and chubby probes reported in Sec. III B). The results of the control experiment are displayed in Fig. 2. When the probe is far away from the substrate and driven at resonance conditions, the estimated lateral oscillation amplitude and equivalent driving force are 1 nm and 50 nN, respectively.^{24,25} This initial value of the resonance frequency is selected as the constant driving frequency of the QTF during the approach and retraction. Notice that the amplitude decreases monotonically but at, respectively, distinct rates in the regions labeled 1, 2, and 3 (the additional three dashed lines drawn along the amplitude trace serve as a reference aid). As the probe begins approaching the sample, at some distance the amplitude starts to decrease. The nominal position $d = 0$ nm has been arbitrarily defined that way. The approaching curve of the probe's amplitude signal in the control experiment displays a longer probe-substrate interaction range (the trace looks a bit inclined already at the 25 nm probe-sample distance) compared with the traces to be reported in Fig. 3²⁷ (where the trace is flat at the 25 nm probe-sample distance). This is attributed to the applied bias voltage in the control-experiment case.²⁸ Long range

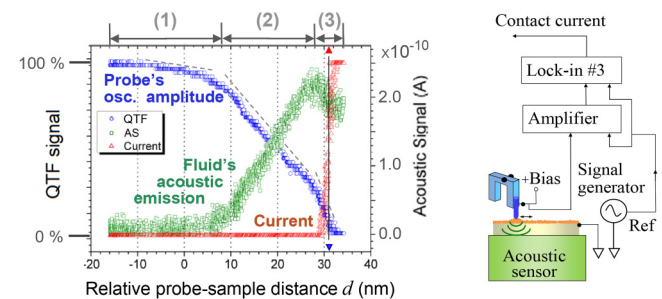
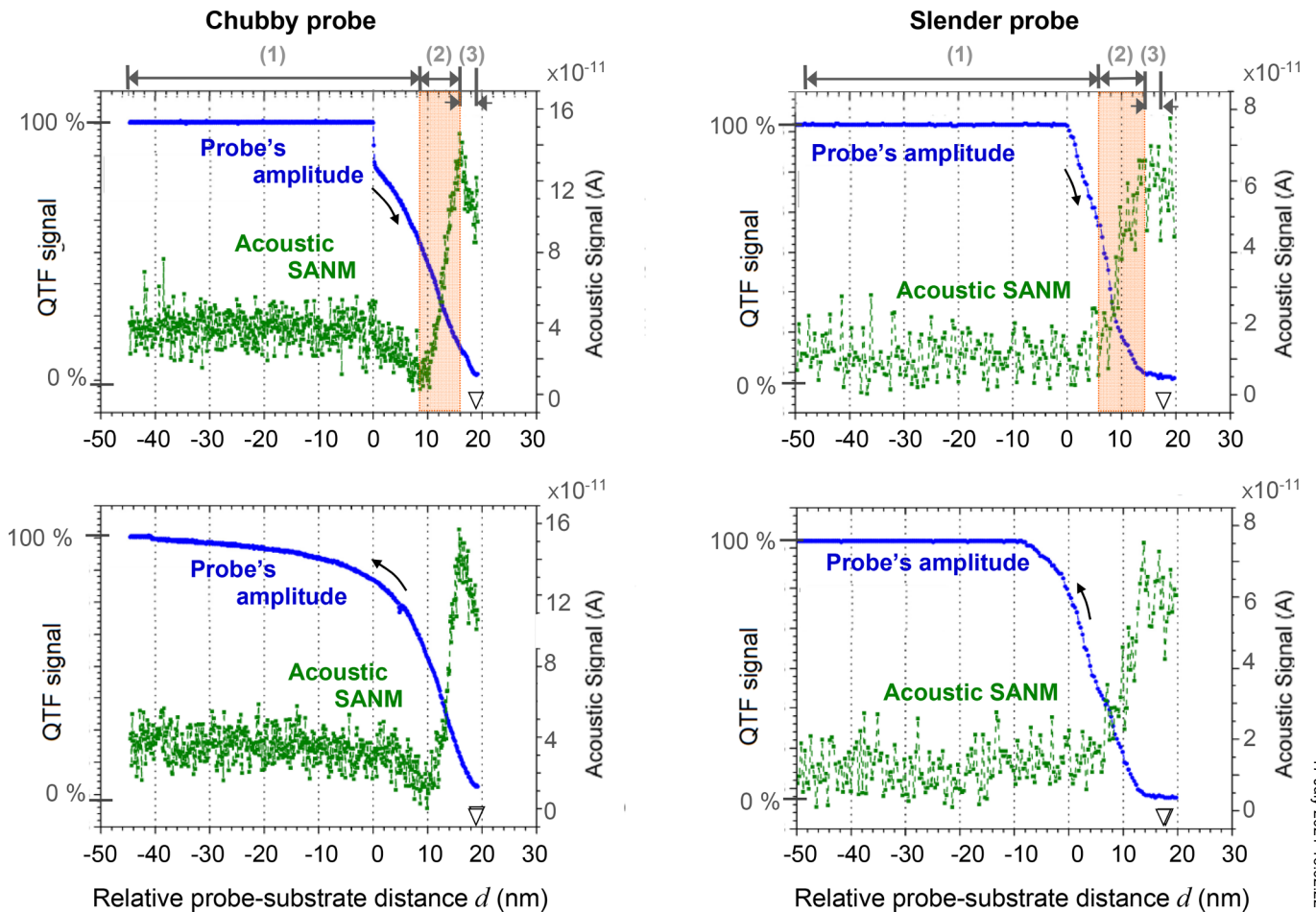


FIG. 2. Left: traces of the probe's lateral oscillation amplitude (QTF signal, left vertical scale), the water meniscus' near-field acoustic emission (indicated by the output current from the acoustic sensor; right side vertical scale), and the probe-sample contact current, as a metallic probe approaches a metallic sample. Right: the contact current circuit added to the setup of Fig. 1.

17 July 2024 16:02:22



17 July 2024 16:02:22

FIG. 3. Approach (top) and retraction (bottom) traces of the gold probe's amplitude (QTF) and the fluid's near-field acoustic emission (SANM) signals acquired with chubby (left) and sharp (right) probes on a (piranha cleaned) hydrophilic silicon oxide substrate, at 25% relative humidity. This set of data belongs to the first group of traces acquired with a freshly prepared probe.²⁷

electrostatic effects are also observed in AFM experiments, where sometimes, a bias voltage between the probe and the sample is purposely applied to counteract the effect.²⁹ At the other extreme of the traces location of the substrate is revealed, as expected, by a rapid increment of the contact current (notice the good correlation between the zero-amplitude of oscillations and the saturation current at the nominal position $d = 31$ nm).³⁰

On the other hand, no acoustic signal is detected in region-1; only at the nominal position $d = 10$ nm (defined as the beginning of region-2) an acoustic signal is detected, suggesting that a water meniscus has just been formed at this probe-sample separation distance (this claim will be further justified below in more detail with additional experimental results). Upon further approach, the near-field acoustic emission from the fluid increases monotonically (even though the probe's amplitude keeps decreasing) and peaks before the probe's amplitude reaches zero. Overall, the acoustic trace in Fig. 2 furnishes a helpful reference trace shape for

comparison purposes with traces to be obtained when testing non-conducting samples, where identification of the surface location is typically less certain.

B. Near-field acoustic emission driven by probes of different tapered geometries

The results obtained using a metallic probe and a hydrophilic silicon oxide substrate are described next. The experiments are performed at 25% relative humidity. First, a chubby (slender) gold probe is placed far away from the sample, where synchronous measurements of its frequency response reveal a $Q = 260$ (485) mechanical quality factor, 3.2 nm (2.4 nm) resonant amplitude of oscillations, corresponding to 220 nN (130 nN) driving force. Subsequently, the probe moves vertically toward the sample at 1.5 nm/s speed. The resulting approach/retraction traces are shown in Fig. 3, which reveals again three distinct regions of interaction

(like the three regions observed in Fig. 2). The magnitude of the acoustic signal level in Fig. 3 is lower than the one displayed in Fig. 2 (these two sets of data were acquired at different days and correspond to different samples,) which can be attributed to unintentional variations in the very thin layer of high-vacuum grease that is applied (sandwiched between the bottom surface of the sample and the top surface of the acoustic sensor) to improve the acoustic signal coupling.³¹

C. Correlation between larger probe's apex area and the increased likelihood of filament bridge formation

Notice that the approaching trace for the chubby probe (displayed on the top-left side of Fig. 3) shows an abrupt decrease in its lateral oscillation amplitude during the trip through region-1; this occurs at the vertical position arbitrarily defined as $d=0$. Such a feature is not observed in the trace for the slender probe (top-right diagram), whose transition from constant-amplitude toward decreasing-amplitude trend is rather smooth. It turns out that a similar approaching-trace behavior (with sudden jumps in the probe's dynamic response) is typically observed in atomic force microscopy.³² In the latter, a plausible interpretation attributes the sudden changes to capillary forces (acting on the relatively weak AFM-cantilever of spring constant, typically 40 N/m or lower) exerted by finger-like water bridges (similar to the ones schematically shown in Fig. 4).³³ It is argued that these filaments stochastically form (between the gaps of multiple discrete asperities present on both the probe and the sample) when the two solid boundaries are sufficiently close (nanometer range) to each other.³⁴ This explanation borrows arguments from stochastic phenomena models used in the description of interfacial friction phenomena,³⁴ which claim that thermally activated mechanisms are involved in the nucleation of capillary bridges across the vertical gap between asperities distributed on the confining sliding surfaces. Similar capillary phenomena may occur then in the SANM set up, but their effects will be on the lateral motion of the probe (the QTF probe holding the probe is rigidly held by the microscope frame, so sudden vertical jumps are discarded). Under this interpretation, the sudden change in amplitude experienced by the chubby probe during the approach process (as observed in Fig. 3) reflects a higher probability for the formation of fluid filament bridges when using probes of a larger apex area. On the other hand, such a sudden change feature is not observed in the corresponding retraction

amplitude trace in Fig. 3, which emphasizes the typical hysteresis observed in these approach/retraction experiments. The smooth characteristic of a retraction trace can be attributed to the gradual elongation (i.e., absence of abrupt changes) of the water meniscus surrounding the probe (the presence of the water meniscus during the retraction is justified in Section III D).³⁵ The volume of the water meniscus (commensurate with the size of the probe's apex) also contributes to the hysteresis. In effect, notice that the chubby probe's gradual retraction trace extends more than the slender counterpart because of the greater volume of the water meniscus.

D. Onset of water meniscus formation and acoustic emission

As the probe further approaches the sample through region-1, the number of discrete finger-like bridges may increase and, thus, cause an increasing damping effect, which explains the monotonic decrease in the probe's lateral oscillation amplitude during the approach. Incidentally, notice that no acoustic signal is detected across region-1 but until $d=9$ nm ($d=8$ nm) in the case of the chubby (slender) probe (a position that defines the beginning of region-2). This result suggests that at this probe-sample distance, the multiple finger-like bridges (accumulated during the trip through region-1) coalesce into a single bulk water meniscus; the latter being able to emit a sustained acoustic wave. A similar interpretation that water condensation is preceded by preliminary transitional states is supported by numerical simulations,³⁶ where it is reported that capillary condensation is preceded by accumulation of a dense vapor between the confining surfaces; likewise, Grand Canonical Monte Carlo simulations report the formation of a chain of hydrogen bonds between the probe and sample as the separation gap reduces.³⁷ SANM adopts then the interpretation that region-1 constitutes a transition region preceding the condensation of a fluid meniscus, after which acoustic emission occurs (see Fig. 4). This acoustic wave, generated at the fluid meniscus, couples to the sample and, subsequently, reaches the acoustic detector located on the back side of the sample.¹⁵ As the approach continues through region-2 (where the probe is *not* in mechanical contact with the substrate), it is observed that the probe's amplitude keeps decreasing while the acoustic signal increases. Thus, SANM helps to identify the near-field acoustic emission from the water meniscus as one of the energy dissipation channels in shear surface interactions.^{38,39}

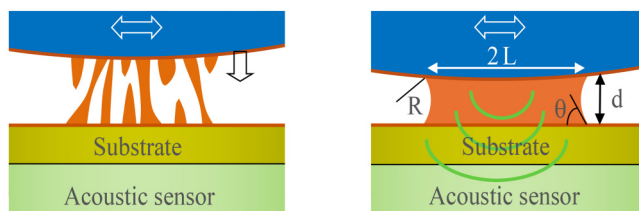


FIG. 4. Left: precursor formation of finger-like bridges between asperities on the probe and the substrate, prior to their coalescence into a bulk meniscus.³⁴ No acoustic emission is detected. Right: formation of a water meniscus as two parallel solid boundaries get closer to each other at a sufficient distance d ;³³ acoustic emission from the meniscus is detected while the probe oscillates laterally.

E. Thermodynamic argument justifying the stochastic formation of a water meniscus

To further support that acoustic emission is not the result of an eventual mechanical contact (of the laterally oscillating probe against the flat substrate) but from the water meniscus that bridges these two solid boundaries, such a condensation phenomenon occurring at the probe-substrate vapor gap can be put on more solid theoretical grounds. But, to simplify the description and following Ref. 33, let us consider a much simpler scenario comprising two parallel plates separated by a distance d and let us find the conditions for water condensation to occur.³³ The right side of Fig. 4 shows a cylindrically symmetric liquid condensate of diameter $2L$; the liquid-substrate contact angle is θ_c and R is the radius of curvature of the condensate's surface in the vertical direction.

17 July 2024 16:02:22

- (a) The change in the bulk grand potential $\Phi(T, V, \mu) = -PV$ of replacing a slab of vapor of thickness d by a slab of liquid is $\Delta\Phi = (-P_{\text{liq}} V_{\text{liq}}) - (-P_{\text{vap}} V_{\text{vap}}) = (P_{\text{vap}} - P_{\text{liq}})(\pi L^2) d$.
- (b) When adding the surface energy term to the grand potential,^{40,41} the increment due to the addition of the liquid plug is

$$\Delta\Phi = \underbrace{2(\pi L^2)(\sigma_{\text{sl}} - \sigma_{\text{sv}})}_{\text{Surface energy term}} + \underbrace{(P_{\text{vap}} - P_{\text{liq}})(\pi L^2)d}_{\text{bulk energy term}}. \quad (1)$$

The second term on the right side of (1) is positive and, thus, represents an energy barrier to overcome if the liquid slab were to be formed. In fact, that term has been used in thermally activated water bridge nucleation models to describe the effects of capillary condensation in friction phenomena.⁴² On the other hand, for a smaller finite value of d , if the surface tension σ_{sl} of the wet solid surface is lower than the surface tension σ_{sv} of the dry solid surface, then the solid favors liquid condensation. The two terms on the right side of expression (1) compete then in the formation of a liquid meniscus. One can see that for a large value of d , an equilibrium condition could not be reached. But for a sufficiently small d , the condition $\Delta\Omega = 0$ for the coexistence of vapor and the fluid plug is fulfilled,

$$-2(\sigma_{\text{sl}} - \sigma_{\text{sv}}) = (P_{\text{vap}} - P_{\text{liq}})d. \quad (2)$$

- (c) In Fig. 4, Young's equation for the contact angle can be written as $\sigma_{\text{lv}} \cos \theta + \sigma_{\text{sl}} = \sigma_{\text{sv}}$. Relation (2) becomes $2\sigma_{\text{lv}} \cos \theta = (P_{\text{vap}} - P_{\text{liq}})d$.
- (d) Let us use the Gibbs–Duhem relationship $d\mu = -s dT + (V/N) dp = -s dT + (1/n) dp$, in order to connect these pressures to the chemical potentials. At a constant temperature, expanding the pressures for small departures $\Delta\mu$ from their common value at the reference saturated condition, $P_{\text{vap}} = P_{\text{sat}} + n_{\text{v}} \Delta\mu$ and $P_{\text{liq}} = P_{\text{sat}} + n_{\text{liq}} \Delta\mu$; hence, $P_{\text{vap}} - P_{\text{liq}} = -(n_{\text{liq}} - n_{\text{vap}}) \Delta\mu$.

$$2\sigma_{\text{lv}} \cos \theta = -(n_{\text{liq}} - n_{\text{vap}}) \Delta\mu d, \quad (3)$$

where n_{liq} and n_{vap} are the liquid and vapor number densities, respectively.

In Eq. (3), for $\Delta\mu$, one can use the change in the chemical potential of the fluid or the vapor. Opting for the latter, $\Delta\mu = kT \ln(P_{\text{vapor}}/P_{\text{sat}})$ leads to an expression for the distance between the plates required for the condensation of a fluid meniscus to occur,

$$d = \frac{2\sigma_{\text{lv}} \cos \theta}{-(n_{\text{liq}} - n_{\text{vap}})kT \ln(P_{\text{vap}}/P_{\text{sat}})}. \quad (4)$$

At 50% humidity, d is of the order of just a few nanometers.⁴³

Although expression (4) provides values that fall within the order of magnitude (nanometers) of experimental observations, additional intervening factors may contribute to the formation of the water meniscus. For example, when using probes of tapered geometry, strong electric fields formed around the apex could play an important role.^{44–46}

F. Source of acoustic emission more involved than just the probe geometry

On the other hand, when comparing the acoustic traces for the chubby and slender probes in Fig. 3, the former shows a decrease in intensity across region-1, which is not observed in the latter. This difference is not fundamental; it can be explained by first noticing that the acoustic signal of the chubby probe displays a non-zero background level, which is present even when the tip is away from the substrate. This is attributed to far-field standing waves in the surrounding ambient air generated by the oscillating QTF.⁴⁷ Once the probe starts to interact with the fluid (at the nominal position $d=0$ in the approaching trace), this background acoustic signal decreases because the probe's amplitude decreases. (This assessment is validated by experiments performed with a probe immersed in bulk water media, where the SAM signal is found to be proportional to the probe's amplitude.⁴⁸) The acoustic trace in region-1 for the slender probe does not change simply because the background acoustic signal is already at a minimum to begin with.

In region-2, the deeper the probe immerses into the meniscus (whose volume is expected to remain constant¹¹), the stronger the acoustic signal. Notice that acoustic emission from the water meniscus around the slender probe is 50% weaker than the fluid around the chubby probe, likely related to its lower volume. (Its shorter retraction-trace path also supports this claim.) However, a 50% decrease in acoustic emission is not commensurate with the five times smaller size of the slender probe (Fig. 1). Hence, explaining the variation of the acoustic signal may be more involved than being associated with just the probe's apex size. In particular, it could be related to the change in the curvature of the meniscus (and its associated change in Laplace pressure) upon variations of the probe-sample distance. Further tests to corroborate this hypothesis are currently being implemented in our laboratory. Other than that, the behavior of the acoustic trace in regions (2) and (3) in Fig. 3 is similar to the one displayed in Fig. 2. Overall, these results show competition between the damping component of shear interactions (causing the probe's amplitude to decrease, and thus, also making the acoustic signal to decrease) and the elastic component of shear interactions (causing the emission of near-field acoustic waves by the mesoscopic meniscus), as the probe approaches the substrate. In this context, the decrease of the acoustic SANM signal in ~ 4 nm-sized region-3 can be attributed to the overwhelming increasing damping force at very short probe-sample distances. The current signal-to-noise ratio of the acoustic signal does not allow to discern the potential presence of solidified water layer(s) on the substrate³⁶ or evaluate the dynamics solidification attributed to the last four water layers (the size of one molecular water layer is 0.25 nm).¹³

IV. CONCLUSION

In summary, shear-force acoustic near-field microscopy (SANM) has been used to monitor acoustic emission from the water meniscus that stochastically forms when the apex of a laterally oscillating tapered probe is placed near a flat sample. The experimental results support the hypothesis that, as the probe approaches the flat sample, first, a number of thin

finger-like water bridges are formed between the discrete asperities on the probe and sample. These finger bridges (more likely to form on wider apex probes) cause damping effects on the probe but are unable to produce sound. Upon further approach, these fingers coalesce into a water meniscus, whose acoustic emission increases despite a decrease in the probe's oscillation amplitude as the probe-sample distance decreases. The use of probes of different apex sizes allowed to identify a lack of proportionality between the intensity of the emitted acoustic signal and the size of their corresponding water meniscus volume, leading to a plausible hypothesis that rather the changing morphology of the meniscus (hence, the change in the Laplace pressure) may play an important role in the SANM signal. SANM brings near-field acoustic sensing capabilities to the study of surface shear interactions. Near-field Acoustic emission accounts for an elastic energy dissipation channel in interfacial friction phenomena.

ACKNOWLEDGMENTS

A.H.L.R. would like to acknowledge the hospitality offered by the National University of Engineering, Lima-Peru (where the final stages of writing this manuscript took place) and the valuable discussions with the local scientists participating (together with AHLR) in the Doctorate Program in Sciences with a Major in Physics. Further recognition to the PDFAXL Faculty Support program from Portland State University. The authors also thank the reviewers for their helpful comments and recommendations.

AUTHOR DECLARATIONS

Conflict of Interest

The authors have no conflicts to disclose.

Author Contributions

Xiaohua Wang: Writing – original draft (equal). **Rodolfo Fernandez:** Software (lead); Validation (equal); Writing – review & editing (supporting). **Theodore Brockman:** Resources (equal); Validation (equal); Writing – review & editing (supporting). **Kacharat Supichayangoon:** Formal analysis (equal); Validation (equal); Writing – review & editing (supporting). **Andres H. La Rosa:** Writing – review & editing (equal).

DATA AVAILABILITY

The data that support the findings of this study are available within the article.

REFERENCES

- ¹K. B. Jinesh and J. W. M. Frenken, "Capillary condensation in atomic scale friction: How water acts like a glue," *Phys. Rev. Lett.* **96**, 166103 (2006).
- ²S. H. Khan and P. M. Hoffmann, "Squeeze-out dynamics of nanoconfined water: A detailed nanomechanical study," *Phys. Rev. E* **92**, 042403 (2015).
- ³P. H. A. Anjos, E. O. Dias, L. Dias, and J. A. Miranda, "Adhesion force in fluids: Effects of fingering, wetting, and viscous normal stresses," *Phys. Rev. E* **91**, 013003 (2015).
- ⁴T. M. Squires and S. R. Quake, "Microfluidics: Fluid physics at the nanoliter scale," *Rev. Mod. Phys.* **77**, 977 (2005).

- ⁵D. Schäffel, K. Koynov, D. Vollmer, H. Butt, and C. Schönecke, "Local flow field and slip length of superhydrophobic surfaces," *Phys. Rev. Lett.* **116**, 134501 (2016).
- ⁶K. Karrai and I. Tiemann, "Interfacial shear force microscopy," *Phys. Rev. B* **62**, 13174 (2000).
- ⁷C. E. Colosqui, M. E. Kavousanakis, A. G. Papathanasiou, and I. E. Kevrekidis, "Mesoscopic model for microscale hydrodynamics and interfacial phenomena: Slip, films, and contact-angle hysteresis," *Phys. Rev. E* **87**, 013302 (2013).
- ⁸M. D. Ma, L. Shen, J. Sheridan, J. Z. Liu, C. Chen, and Q. Zheng, "Friction of water slipping in carbon nanotubes," *Phys. Rev. E* **83**, 036316 (2011).
- ⁹J. Israelachvili and M. Ruths, "Brief history of intermolecular and intersurface forces in complex fluid systems," *Langmuir* **29**, 9605 (2013).
- ¹⁰A. Mukhopadhyay, S. C. Bae, J. Zhao, and S. Granick, "How confined lubricants diffuse during shear," *Phys. Rev. Lett.* **93**, 236105 (2004).
- ¹¹L. Sirghi, R. Szożkiewicz, and E. Riedo, "Volume of a nanoscale water bridge," *Langmuir* **22**, 1093 (2006).
- ¹²M. U. Hammer, T. H. Anderson, A. Chaimovich, M. S. Shell, and J. Israelachvili, "The search for the hydrophobic force law," *Faraday Discuss* **146**, 299 (2010).
- ¹³S. H. Khan, G. Matei, S. Patil, and P. M. Hoffmann, "Dynamic solidification in nanoconfined water films," *Phys. Rev. Lett.* **105**, 106101 (2010).
- ¹⁴A. La Rosa, X. Cui, J. McCollum, N. Li, and R. Nordstrom, "The ultrasonic/shear-force microscope: Integrating ultrasonic sensing into a near-field scanning optical microscope," *Rev. Sci. Instrum.* **76**, 093707 (2005).
- ¹⁵The SANM sensor is placed in intimate mechanical contact with the back side of the substrate. As a reference, the speed of sound in water is ~ 1480 m/s (in solids is ~ 5000 m/s); at 32 kHz, the corresponding wavelength is 4.5 cm (~ 15 cm in solids). Since the water gap is a few nanometers and the substrate thickness in our experiments is of the order of ~ 2 mm, the acoustic detection is within the realm of the near field region.
- ¹⁶B. Ren, G. Picardi, and B. Pettinger, "Preparation of gold tips suitable for tip-enhanced Raman spectroscopy and light emission by electrochemical etching," *Rev. Sci. Instrum.* **75**, 837 (2004). We used Au wire, purity 99.95%, ESPI Inc.
- ¹⁷M. Luna, J. Colchero, A. Gil, J. Gómez-Herrero, and A. M. Baro, "Application of non-contact scanning force microscopy to the study of water adsorption on graphite, gold and mica," *Appl. Surf. Sci.* **157**, 393 (2000).
- ¹⁸T. Smith, "The hydrophilic nature of a clean gold surface," *J. Colloid Interface Sci.* **75**, 51 (1980).
- ¹⁹The hydrophobic or hydrophilic character of the probe affects the results, which we plan to report in more detail in a separate manuscript.
- ²⁰S. Kaya, P. Rajan, H. Dasari, D. C. Ingram, W. Jadwisieniczak, and F. Rahman, "A systematic study of plasma activation of silicon surfaces for self-assembly," *ACS Appl. Mater. Interfaces* **7**, 25024 (2015).
- ²¹D. B. Asay and S. H. Kim, "Evolution of the adsorbed water layer structure on silicon oxide at room temperature," *J. Phys. Chem. B* **109**, 16760 (2005).
- ²²For the results reported herein were obtained using a SE40-Q sensor, Dunegan Engineering Consultants. (Since that sensor is currently out of stock, an alternative is the VS30-V AE sensor; Acoustic Technology Group, Michigan, USA).
- ²³Nano-OP65 (Mad City Labs, Inc.) that provides a $60\text{ }\mu\text{m}$ travel range with nanometer precision; a close loop feedback control eliminates hysteresis effects.
- ²⁴J. Rychen, T. Ihn, P. Studerus, A. Herrmann, K. Ensslin, H. J. Hug, P. J. A. van Schendel, and H. J. Güntherodt, "Operation characteristics of piezoelectric quartz tuning forks in high magnetic fields at liquid helium temperatures," *Rev. Sci. Instrum.* **71**, 1695 (2000).
- ²⁵A quantitative estimation of the probe's oscillation amplitude u is obtained by applying the harmonic approximation model (as described in Ref. 24), which gives a relationship of $\Delta I = 10$ nA rms when the amplitude is $u_0 = 4$ nm rms. This conversion is also calculated in Ref. 14 (see Ref. 18 cited there).
- ²⁶The current preamplifier SR570 (Stanford Research System) not only detects the current but also allows the application of a DC bias voltage to the probe. The conducting sample is obtained by sputter coating a thin layer of gold (30 nm thick) onto a silicon oxide substrate.

17 July 2024 16:02:22

- ²⁷We have observed that the initial approaching traces (using a freshly prepared probe) tend to be different than the ones obtained after many approach/retraction trials. For example, the abrupt change in the approaching trace of the chubby probe tend to disappear. It is plausible to attribute this behavior to a progressively less dry condition of the probe after several approach/retraction trips where, each time, it encounters a water meniscus.
- ²⁸The longer interaction range of the probe's amplitude detected when using a bias voltage across conductive probe and substrate has been consistently verified in other similar experiments in our laboratory.
- ²⁹Y. Sugimoto, P. Pou, M. Abe, P. Jelinek, R. Perez, S. Morita, and O. Custance, "Chemical identification of individual surface atoms by atomic force microscopy," *Nature* **446**, 64 (2007).
- ³⁰The absence of a sharp transition in the contact current can be attributed to the probe tapping progressively more and more against the substrate (since the lateral oscillations are not perfectly parallel to the substrate).
- ³¹It must be mentioned, however, that in a separate control experiment (not detailed here), a singular sample was prepared with a top surface comprising contiguous (but separated) conductive and bare glass regions. In consequence, since both regions had a common bottom surface, their coupling to the acoustic sensor was the same. For such a sample, it was found that the acoustic signal through the metallic region was consistently greater than through the glass region. We are investigating further such a preliminary result.
- ³²S. Rozhok, P. Sun, R. Piner, M. Lieberman, and C. A. Mirkin, "AFM study of water meniscus formation between an AFM tip and NaCl substrate," *J. Phys. Chem. B* **108**, 7814 (2004).
- ³³W. F. Saam, "Wetting, capillary condensation and more," *J. Low Temp. Phys.* **157**, 77 (2009).
- ³⁴I. Barel, A. E. Filippov, and M. Urbakh, "Formation and rupture of capillary bridges in atomic scale friction," *J. Chem. Phys.* **137**, 164706 (2012).
- ³⁵A sudden change at the end of the retraction retrace is sometimes observed. This is attributed to the hydrodynamic instability (driven by the Laplace pressure) that occurs when the neck of the meniscus becomes very thin in the last stage of the probe's retraction from the substrate.
- ³⁶W. J. Stroud, J. E. Curry, and J. H. Cushman, "Capillary condensation and snap-off in nanoscale contacts," *Langmuir* **17**, 688 (2001).
- ³⁷R. C. Major, J. E. Houston, M. J. McGrath, J. I. Siepmann, and X.-Y. Zhu, "Viscous water meniscus under nanoconfinement," *Phys. Rev. Lett.* **96**, 177803 (2006).
- ³⁸Our group has also identified another (far-field) acoustic energy dissipation channel in probe-sample shear interaction (that couples to the holder of the probe), as described in more detail in Ref. 39.
- ³⁹A. H. La Rosa, N. Li, R. Fernandez, X. Wang, R. Nordstrom, and S. K. Padigi, "Whispering-gallery acoustic sensing: Characterization of mesoscopic films and scanning probe microscopy applications," *Rev. Sci. Instrum.* **82**, 093704 (2011).
- ⁴⁰R. Evans, "Fluids adsorbed in narrow pores: Phase equilibria and structure," *J. Phys.: Condens. Matter* **2**, 8989 (1990).
- ⁴¹E. Charlaix and M. Ciccotti, "Capillary condensation in confined media," in *Handbook of Nanophysics Principles and Methods*, edited by K. D. Sattler (CRC Press, 2017), Chap. 12.
- ⁴²E. Riedo, F. Lévy, and H. Brune, "Kinetics of capillary condensation in nanoscopic sliding friction," *Phys. Rev. Lett.* **88**, 185505 (2002).
- ⁴³Using $\sigma_{lv} = 72 \text{ mN/m} = 0.072 \text{ J/m}^2$, $n_{liq} = 33.3 \times 10^{27}/\text{m}^3$, kT at 300 K $\sim 0.025 \text{ eV}$. At 50% humidity expression (5) gives $d = 1.5 \text{ nm}$.
- ⁴⁴R. Garcia and M. Calleja, "Patterning of silicon surfaces with noncontact atomic force microscopy: Field-induced formation of nanometer size water bridges," *J. Appl. Phys.* **86**, 1898 (1999).
- ⁴⁵A. Garcia-Martin and R. Garcia, "Formation of nanoscale liquid menisci in electric fields," *Appl. Phys. Lett.* **88**, 123115 (2006).
- ⁴⁶T. Cramer, F. Zerbetto, and R. Garcia, "Molecular mechanism of water bridge buildup: Field-induced formation of nanoscale menisci," *Langmuir* **24**, 6116–6120 (2008).
- ⁴⁷Typically an acoustic standing wave, generated by the laterally oscillating probe in the air medium between the flat sample stage and the flat disk plate of the SANM microscope head-stage, is sensitively picked up by the acoustic transducer. (In fact, driving the QTF at higher driving voltage allows testing and optimizing the acoustic detection prior to any experiment.) But, since the associated wavelength of the acoustic wave in air is of the order of 1 cm at 32 kHz, this far-field acoustic background does not affect significantly the measurements involving nanometer-sized probe's vertical displacements.
- ⁴⁸X. Wang, R. Fernandez, N. Li, H.-C. Hung, A. Venkataraman, R. Nordstrom, and A. H. La Rosa, "Near-field acousto monitoring shear interactions inside a drop of fluid: The role of the zero-slip condition," *Phys. Fluids* **28**, 052001 (2016).